Orientation-dependent electromagnetic properties of basalt fibre/nickel core–shell heterostructures*

Kang Yu-Qing(康玉清)[a], Cao Mao-Sheng(曹茂盛)[a)†], Yuan Jie(袁 杰)[b)‡], and Fang Xiao-Yong(房晓勇)[a)]

[a)] *School of Materials Science and Engineering, Beijing Institute of Technology, Beijing* 100081, *China*
[b)] *School of Information Engineering, Central University for Nationality, Beijing* 100081, *China*

(Received 21 May 2009; revised manuscript received 26 May 2009)

The influence of orientation on electromagnetic properties of basalt fibre/nickel core–shell heterostructures prepared by a simple electroless plating method is investigated. For comparison, the same investigation is also performed on naked basalt fibres. For electromagnetic measurement, the directions of basalt fibre/nickel and naked basalt fibres are parallel, random and perpendicular to the direction of external electric field, termed $E_{||}$ sample, random sample and $E_{\perp}$ sample, respectively. Electromagnetic anisotropy can be clearly observed in the basalt fibre/nickel core–shell heterostructures, while electromagnetic properties of naked basalt fibres are unrelated to the orientation. The $E_{\perp}$ basalt fibre/nickel shows the highest dielectric loss but the lowest magnetic loss, and $E_{||}$ basalt fibre/nickel exhibits the highest magnetic loss but the lowest dielectric loss. The dielectric loss of $E_{\perp}$ basalt fibre/nickel is several times as large as that of $E_{||}$ basalt fibre/nickel, which could be attributed to the increase of polarization relaxation time as a consequence of the nanosize-confinement effect. The magnetic loss of $E_{||}$ basalt fibre/nickel is even one order of magnitude higher than that of $E_{\perp}$ basalt fibre/nickel, which originates mainly from the natural magnetic resonance of basalt fibre/nickel core–shell heterostructures.

Keywords: one-dimensional materials, heterostructure, electromagnetic property, orientation

PACC: 7740, 8110D

1. Introduction

In recent years, core–shell heterostructures, especially one-dimensional (1D) core–shell heterostructures, have attracted a great deal of attention due to their fascinating optical, electronic, or magnetic properties.[1−4] Many researchers have reported on the preparation of 1D core–shell heterostructures, and the potential applications in fields such as electronics, magnetism, optics, and biomedicine.[5−11] More recently, considerable attention has been paid to the electromagnetic properties of 1D core–shell heterostructures, such as CNTs/Fe,[12] CNTs/$CoFe_2O_4$,[13] CdS/α-Fe_2O_3,[14] and so on.[15−20] These core–shell structures, which exhibit better electromagnetic properties than pure core or shell materials, could be a good candidate for a microwave absorption device application. Moreover, it is believed that the electromagnetic properties of 1D core–shell heterostructures are relative to the orientation due to the anisotropic geometries. Thus, it is significant to research the orientation influence on electromagnetic properties of 1D core–shell heterostructures for further application.

Orientation-dependent properties of crystals, ceramics, and metal alloys have been extensively investigated.[21−23] Recently, with the development of nanoscience and nanotechnology, many efforts have been made to study the orientation-dependent properties of nanomaterials with anisotropic geometries.[24−31] However, these studies mainly focus on the orientation dependence of dielectric or ferroelectric properties of thin films.[24,26−28] Up to now, little research has been reported on the orientation-dependent electromagnetic properties of 1D core–shell heterostructures, which would be favourable to the application of 1D core–shell heterostructures as microwave absorption materials. In this work, the electromagnetic properties of basalt fibre/nickel (BF/Ni) core–shell heterostructures as well as naked

*Project supported by the National Natural Science Foundation of China (Grant No. 50872159), the National Defense Pre-Research Foundation of China (Grant Nos. 513180303 and A2220061080), and the Specialized Research Fund for the Doctoral Program of Higher Education of China (Grant No. 2004007021).
†Corresponding author. E-mail: caomaosheng@bit.edu.cn
‡E-mail: yuanjie4000@sina.com
© 2010 Chinese Physical Society and IOP Publishing Ltd

basalt fibres (BFs) with different orientations are investigated. The BF/Ni core–shell structures exhibit obvious orientation-dependent electromagnetic properties, while electromagnetic properties of naked BF are unrelated to the orientation. Moreover, the mechanism of the orientation-dependent electromagnetic properties of the BF/Ni core–shell heterostructures is discussed.

2. Experimental details

Cut BFs, with an average diameter of 9 μm and average length of 1 cm, were used in the experiment. The electroless plating approach was employed to prepare the BF/Ni core–shell heterostructures. Prior to electroless plating, a pre-treatment process was performed by introducing the naked BF into HF/HCl solution, $SnCl_2$ solution, and $PdCl_2$ solution in sequence for the deposition of Pd-Sn catalytic nuclei on the surface of basalt fibres. Then the treated BFs were introduced into the electroless plating solution for the deposition of nickel nanoparticles on the surface of BF. The detailed preparation process of the BF/Ni core–shell heterostructures has been described in our previous work.[32] By the electroless plating approach, a uniform and continuous nanostructured nickel shell was coated on the surface of the BF, forming BF/Ni core–shell heterostructures. The morphologies and the compositions of the BFs and the BF/Ni core–shell heterostructures were investigated by a scanning electron microscope (SEM, HITACHI S-3500N) and energy dispersive spectrum (EDS, OXFORD INCA). For the measurements of electromagnetic properties, the naked BFs and the BF/Ni core–shell structures were dispersed in a paraffin matrix with a weight fraction of 10% and then compacted into a rectangle with dimensions of 22.9 mm×11 mm×2.7 mm to fit the waveguide sample holder for electromagnetic measurements. The permittivity and the permeability were measured by using an ANRIGSU 37269D vector network analyser.

3. Results and discussion

SEM images of the naked BFs and BF/Ni core–shell heterostructures are shown in Fig. 1. From Fig. 1(a), the SEM image of the naked BFs, it can be seen that the surface of naked BFs is very smooth. Figures 1(b) and 1(c) show the SEM image and EDS of BF/Ni core–shell heterostructures. It is clear that the surface of the basalt fibres is coated by a uniform nickel shell after electroless plating. A high-magnification SEM image of the nickel shell indicates that the nickel shell is composed of nanoscale nickel particles with a size of about 20–100 nm as shown in Fig. 1(d). The section image of the BF/Ni core–shell structures shown in Fig. 1(e) indicates that the nickel shell is continuous with a thickness of about 0.5 μm.

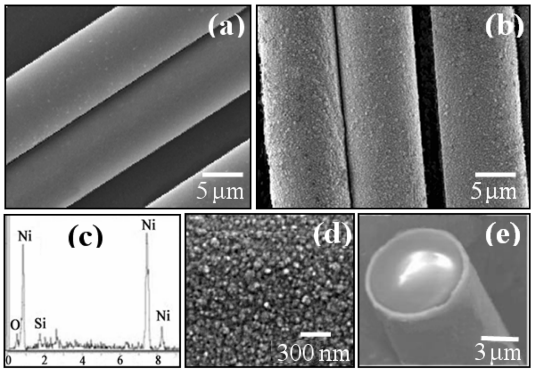


Fig. 1. (a) SEM image of naked basalt fibres, (b) SEM image and (c) EDS of the basalt fibre/nickel core–shell heterostructures; (d) high-magnification SEM image of the nickel shell; (e) the section image of the basalt fibre/nickel core–shell heterostructures.

The electromagnetic properties of naked BF heterostructures and BF/Ni core–shell heterostructures in different orientations were investigated in a range from 8.2 to 12.4 GHz (X band). Figure 2 shows a schematic illustration of samples used for electromagnetic measurement with BFs and BF/Ni core–shell structures in different orientations. The arrow in Fig. 2 shows the direction of the external electric field. From Fig. 2, the directions of BF/Ni and naked BFs arrayed in paraffin are parallel, random and perpendicular to the direction of external electric field, which were termed $E_{||}$ sample, random sample and $E_{\perp}$ sample, respectively. Figure 3 shows the real permittivity (ε') and dielectric loss tangent ($\tan\delta_{\rm e}$) of naked BFs and BF/Ni core–shell structures. For the naked BFs, little difference in ε' and $\tan\delta_{\rm e}$ among the $E_{||}$ sample, random sample and $E_{\perp}$ sample can be found, and their values are found to be ∼2.6 and ∼0.01 in the whole range of frequency investigated, while the values of ε' and $\tan\delta_{\rm e}$ of BF/Ni are highly dependent on the orientation. The average values of ε' of $E_{||}$ BF/Ni, random BF/Ni and $E_{\perp}$ BF/Ni are 6.2, 11.3 and 19.6, respectively. The value of $\tan\delta_{\rm e}$ of $E_{\perp}$ BF/Ni varies from 0.56–0.76 depending on the frequency, which is several times as large as that of $E_{||}$ BF/Ni (0.03–0.33), while for random BF/Ni, the

value of $\tan\delta_e$ is about 0.5 in the whole X band. Figure 4 shows the real permeability (μ') and magnetic loss tangent ($\tan\delta_m$) of BF/Ni core–shell structures. The values of μ' and $\tan\delta_m$ of naked BFs, which is known to be a non-magnetic material, are almost constant in the X band and are not shown in the figure. It is clear that the μ' and $\tan\delta_m$ of BF/Ni are also related to the orientation. The value of $\tan\delta_m$ for $E_{||}$ BF/Ni is even one order of magnitude higher than that of $E_\perp$ BF/Ni. The $\tan\delta_m$ of $E_{||}$ BF/Ni reaches up to ∼5.5, which is much higher than that of Fe encapsulated carbon nanotubes.[12] From these results, electromagnetic anisotropy can be clearly seen in the BF/Ni core–shell structures but not in naked BFs. The $E_\perp$ BF/Ni shows the highest dielectric loss but the lowest magnetic loss, and $E_{||}$ BF/Ni exhibits the highest magnetic loss but the lowest dielectric loss. This is significant for tunable microwave device applications.

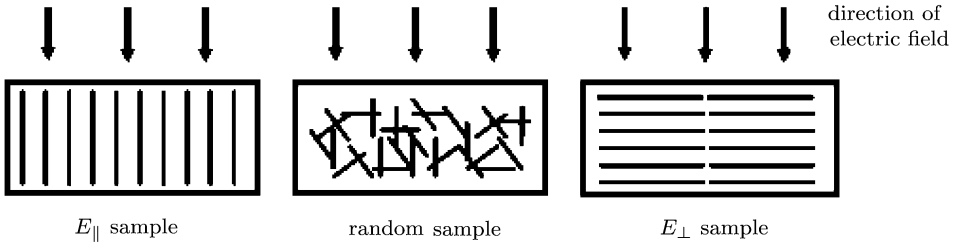


Fig. 2. Schematic illustration of samples used for electromagnetic measurement with basalt fibres and basalt fibre/nickel core–shell structures in different orientations. Arrows show the direction of external electric field.

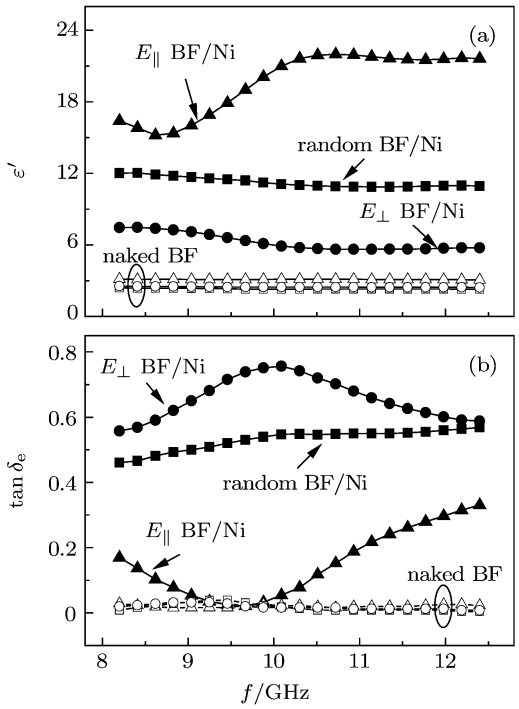


Fig. 3. (a) Real permittivity and (b) dielectric loss tangent of the naked basalt fibres and basalt fibre/nickel core–shell structures with different orientations.

A possible mechanism for the orientation-dependent electromagnetic properties of BF/Ni core–shell structures is described as follows. According to the dielectric physics theory, the dielectric loss of BF/Ni core–shell heterostructures mainly comes from the polarization relaxation between the core/shell interfaces, i.e. Maxwell–Wagner relaxation,[33,34] as a core/shell interface is constructed with BF as core and Ni as shell. For $E_\perp$ BF/Ni, the polarization is lagged due to the small size of the nickel shell along the direction of the external electric field, which leads to the increase of polarization relaxation time. According to Correia and Ramos[35] the dielectric loss of dielectrics increases with polarization relaxation time increasing. So the dielectric loss of $E_\perp$ BF/Ni is higher than those of other samples. From the experimental results, it is clear that the magnetic loss of the BF/Ni core–shell heterostructures originates mainly from the nickel shell. In our case, natural magnetic resonance plays a dominant role in the high magnetic loss of $E_{||}$ BF/Ni core–shell heterostructures. The inset in Fig. 4(b) shows the complex permeability of $E_{||}$ BF/Ni. It reveals that the real part (μ') exhibits an abrupt decrease from 1.69 to 0.14 at 8.2–11 GHz and retains an approximate constant at 11–12.4 GHz. Meanwhile the imaginary part (μ'') increases from 0.68 to 1.44 at 8.2–9.2 GHz and then decreases at high frequencies.

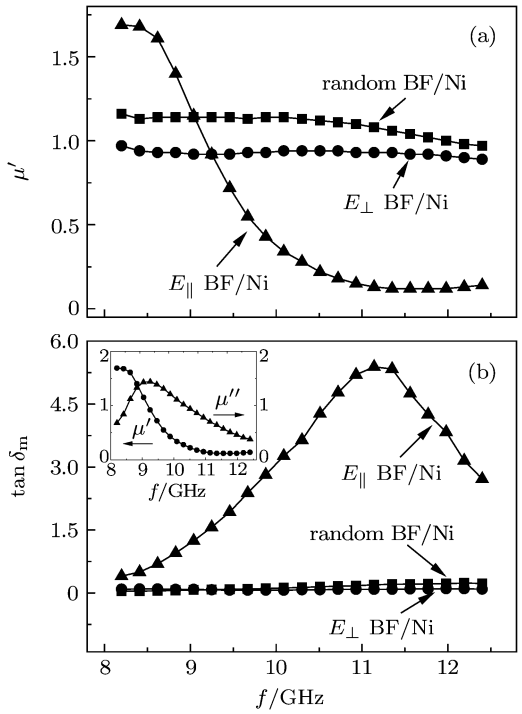


Fig. 4. (a) Real permeability and (b) magnetic loss tangent of the basalt fibre/nickel core–shell structures with different orientations. The inset (b) shows the complex permeability of the $E_{||}$ sample, implying the occurring of natural resonance.

It is interesting that the maximum value of μ'' appears at 9.2 GHz while the value of μ' is approximately 1.0, which implies the natural magnetic resonance occurring in $E_{||}$ BF/Ni. The same phenomenon has also been reported in carbon-coated nickel nanocapsules with a natural resonance frequency of about 5.5 GHz.[36] It was reported that the remarkably increased anisotropic energy that was affected by a very small size effect resulted in the shift of natural resonance frequency to higher frequencies.[37] In the present experiment, the natural resonance frequency of BF/Ni core–shell heterostructures is about 9.2 GHz, which would be significant for their use as electromagnetic wave absorption materials in the microwave range.

4. Conclusions

The influence of orientation on electromagnetic properties of BF/Ni core–shell heterostructures as well as naked BFs is investigated. The electromagnetic properties of BF/Ni core–shell heterostructures are highly dependent on the orientation, while electromagnetic parameters of naked BFs in different orientations show little difference. The $E_\perp$ BF/Ni shows the highest dielectric loss but the lowest magnetic loss, and $E_{||}$ BF/Ni exhibits the highest magnetic loss but the lowest dielectric loss. The values of both dielectric loss and magnetic loss for random BF/Ni lie between those for $E_{||}$ BF/Ni and $E_\perp$ BF/Ni. The high dielectric loss of $E_\perp$ BF/Ni, which is several times as large as that of $E_{||}$ BF/Ni, could be attributed to the increase of polarization relaxation time resulting from the nanosize-confinement effect. The high magnetic loss of $E_{||}$ BF/Ni, which is even one order of magnitude higher than that of $E_\perp$ BF/Ni, originates mainly from the natural magnetic resonance of BF/Ni core–shell heterostructures. This study provides a good candidate for tunable microwave absorption device applications from the BF/Ni core–shell heterostructures.

References

[1] Mao C, Solis D J, Reiss B D, Kottmann S T, Sweeney R Y, Hayhurst A, Georgiou G, Iverson B and Belcher A M 2004 *Science* **303** 213
[2] Xia Y N, Yang P D, Sun Y G, Wu Y Y, Mayers B, Gates B, Yin Y D, Kim F and Yan H Q 2003 *Adv. Mater.* **15** 353
[3] Zou G Z, Cao M S, Lin H B, Jin H B, Kang Y Q and Chen Y J 2006 *Powder Tech.* **168** 84
[4] Zou G Z, Cao M S, Zhang L, Li J G, Xu H and Chen Y J 2006 *Surf. Coat. Tech.* **201** 108
[5] Wang W Z, Zeng B Q, Yang J, Poudel B, Huang J Y, Naughton M J and Ren Z F 2006 *Adv. Mater.* **18** 3275
[6] Zhang X H, Zhang Y, Xu J, Wang Z, Chen X H, Yu D P, Zhang P, Qi H H and Tian Y J 2005 *Appl. Phys. Lett.* **87** 123111
[7] Guo L, Ji Y L, Xu H B, Simon P and Wu Z Y 2002 *J. Am. Chem. Soc.* **124** 14864
[8] Zhang D H, Liu Z Q, Han S, Li C, Lei B, Stewart M P, Tour J M and Zhou C W 2004 *Nano. Lett.* **4** 2151
[9] Chueh Y L, Chou L J and Wang Z L 2006 *Angew. Chem. Int. Ed.* **45** 7773
[10] Chen Y J, Zhu C L, Cao M S and Wang T H 2007 *Nanotechnology* **18** 285502
[11] Chueh Y L, Hsieh C H, Chang M T, Chou L J, Lao C S, Song J H, Gan J Y and Wang Z L 2007 *Adv. Mater.* **19** 143
[12] Che R C, Peng L M, Duan X F, Chen Q and Liang X L 2004 *Adv. Mater.* **16** 401
[13] Che R C, Zhi C Y, Liang C Y and Zhou X G 2006 *Appl. Phys. Lett.* **88** 033105
[14] Shi X L, Cao M S, Yuan J, Zhao Q L, Kang Y Q, Fang X Y and Chen Y J 2008 *Appl. Phys. Lett.* **93** 183118

[15] Long Y Z, Yin Z H, Hui W, Chen Z J and Wan M X 2008 *Chin. Phys.* B **17** 2707

[16] Long Y Z, Li M M, Sui W M, Kong Q S and Zhang L 2009 *Chin. Phys.* B **18** 1221

[17] Wang Q, Li G J, Li D G, Lü X and He J C 2009 *Chin. Phys.* B **18** 1843

[18] Liu G L, Yang Z H and Fang G L 2009 *Acta Phys. Sin.* **58** 3364 (in Chinese)

[19] Zhou Y, Kang Y Q, Fang X Y, Yuan J, Shi X L, Song W L and Cao M S 2008 *Chin. Phys. Lett.* **25** 1902

[20] Zou G Z, Cao M S, Zhang L, Jin H B, Xu H and Wang Z P 2006 *J. Inorg. Mater.* **21** 797

[21] Mao Z Q, He Z H, Chen D H, Cheung W Y and Wong S P 2007 *Solid State Commun.* **142** 329

[22] Knowles K M and Turan S 2000 *Ultramicroscopy* **83** 245

[23] Bickermann M, Epelbaum B M, Heimann P, Herro Z G and Winnacker A 2005 *Appl. Phys. Lett.* **86** 131904

[24] Cheng Z X, Kannan C V, Ozawa K, Kimura H and Wang X L 2006 *Appl. Phys. Lett.* **89** 032901

[25] Cao G X and Chen X 2008 *Int. J. Solids. Struct.* **45** 1730

[26] Zhong X L, Wang J B, Zheng X J, Zhou Y C and Yang G W 2004 *Appl. Phys. Lett.* **85** 5661

[27] Oikawa T, Aratani M, Funakubo H, Saito K and Mizuhira M 2004 *J. Appl. Phys.* **95** 3111

[28] Moon S E, Kim E K, Kwak M H, Ryu H C, Kim Y T, Kang K Y, Lee S J and Kim W J 2003 *Appl. Phys. Lett.* **83** 2166

[29] Gu X K and Cao B Y 2007 *Chin. Phys.* **16** 3777

[30] Ma H, Sun R Z, Li Z X and Liu Y F 2008 *Chin. Phys.* B **17** 255

[31] Deng L G and Luo L Y 2007 *Acta Phys. Sin.* **56** 1480 (in Chinese)

[32] Kang Y Q, Cao M S, Shi X L and Hou Z L 2007 *Surf. Coat. Tech.* **201** 7201

[33] Calame J P, Abe D K, Levush B and Danly B G 2001 *J. Appl. Phys.* **89** 5618

[34] Liu X G, Jiang J J, Geng D Y, Li B Q, Han Z, Liu W and Zhang Z D 2009 *Appl. Phys. Lett.* **94** 053119

[35] Correia N T and Ramos J J M 2000 *Phys. Chem. Chem. Phys.* **2** 5712

[36] Zhang X F, Dong X L, Huang H, Liu Y Y, Wang W N, Zhu X G, Lü B, Lei J P and Lee C G 2006 *Appl. Phys. Lett.* **89** 053115

[37] Chen Y J, Gao P, Wang R X, Zhu C L, Wang L J, Gao M S and Jin H B 2009 *J. Phys. Chem.* C **113** 10061